

DPA-DenseBiasNet: Semi-supervised 3D Fine Renal Artery Segmentation with Dense Biased Network and Deep Priori Anatomy



Yuting He¹, Guanyu Yang^{1,4*}, Yang Chen^{1,4}, Youyong Kong^{1,4}, Jiasong Wu^{1,4}, Lijun Tang³, Xiaomei Zhu³, Jean-Louis Dillenseger^{2,4}, Pengfei Shao⁵, Shaobo Zhang⁵, Huazhong Shu^{1,4}, Jean-Louis Coatrieux², Shuo Li⁶

- 1.LIST, Key Laboratory of Computer Network and Information Integration (Southeast University), Ministry of Education, Nanjing, China
- 2.Univ Rennes, Inserm, LTSI - UMR1099, Rennes, F-35000, France
- 3.Dept. of Radiology, the First Affiliated Hospital of Nanjing Medical University, Nanjing, China
- 4.Centre de Recherche en Information Biomédicale Sino-Françaises (CRIBs)
- 5.Dept. of Urology, the First Affiliated Hospital of Nanjing Medical University, Nanjing, China
- 6.Dept. of Medical Biophysics, University of Western Ontario, London, ON, Canada

☎: +86-25-83794249

✉: yang.list@seu.edu.cn



INTRODUCTION

❖ Task definition

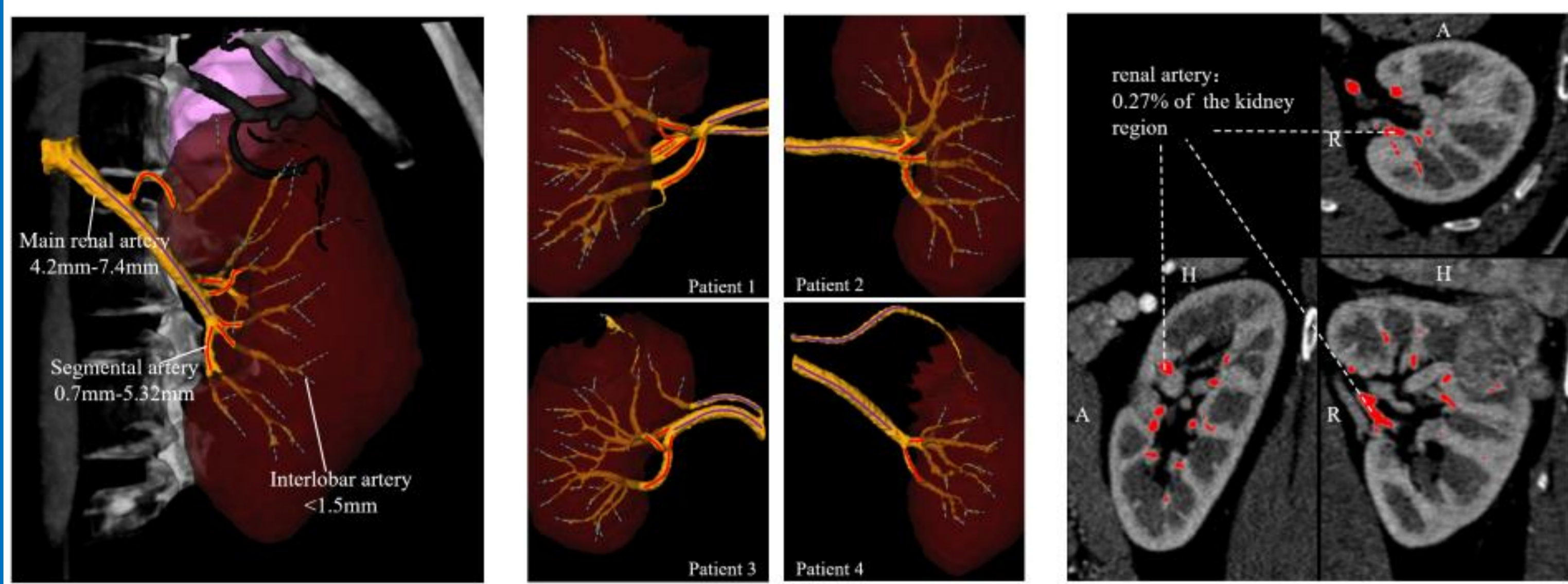
➤ Achieving 3D renal artery tree on abdominal CTA image that reaches the end of interlobar arteries.

❖ Clinical significance

➤ Clinicians locate the blood feeding region corresponding to each interlobar artery easily via this fine renal artery segmentation which is important for the diagnosis and pre-operative planning of kidney disease.

❖ Challenges

- 1) Large intra-scale changes
- 2) Large inter-anatomy variation
- 3) Thin structure
- 4) Small volume ratio
- 5) Limitation of labeled data



a) Large intra-scale changes b) Large inter-anatomy variation c) Small volume ratio & Thin structure
Fig.1 The challenges of 3D fine renal artery segmentation.

METHODOLOGY

❖ Dense biased network for fine segmentation

▪ Advantages

- Simplify the training process
- Adapt to large intra-scale changes

▪ Dense biased connection

➤ Each layer gets a part of feature maps from all preceding layers as additional inputs and transmits a part of its output feature maps to all forward layers, as is shown in Fig.2(d).

$$\text{➤ } F_l = H_l(F_{l-1} \circ F_{l-2}[0 : k_{l-2}] \circ \dots \circ F_0[0 : k_0])$$

▪ DenseBiasNet

➤ As shown in Fig.2(a), It comprises of 14 3D convolution layers, 3 maxpooling layers, 3 3D deconvolution layers used to change scales and a $1 \times 1 \times 1$ convolution layer followed a softmax as the output layer to reduce the number of channels to classes. The dense biased connection is used throughout the network to adapt to different scale arteries.

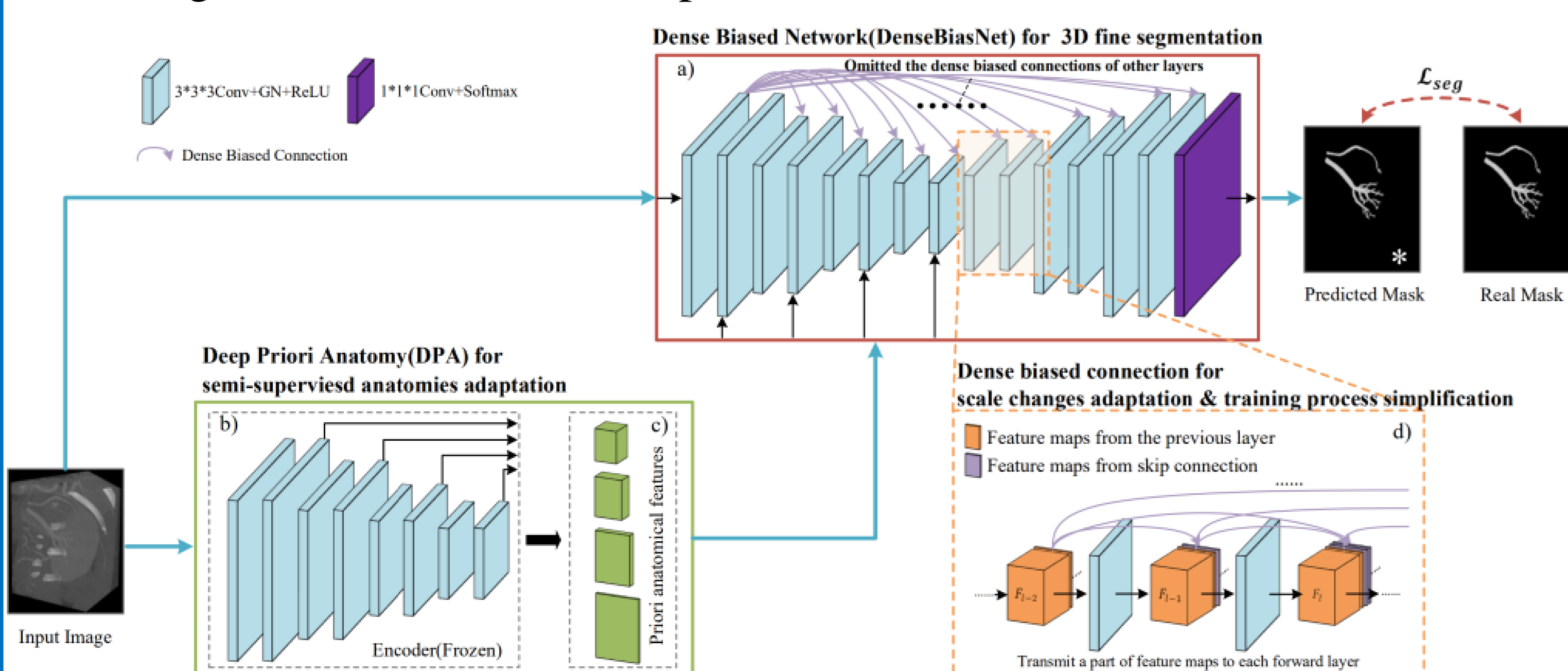


Fig.2 The framework of DPA-DenseBiasNet.

❖ Deep priori anatomy based semi-supervised learning

▪ Advantages

- Adapts to more anatomical structures
- Focuses on both local and global anatomical information
- Improves the network's generalization ability
- Suitable for thin structures

▪ DPA for semi-supervised anatomical adaptation

➤ A convolutional denoising autoencoder was trained with numerous unlabeled data, and then its encoder part was frozen and used to extract anatomical features (Fig. 2(b))

EXPERIMENTS

❖ Dataset

➤ Abdominal contrast-enhanced CT images of 170 patients who underwent LPN surgery were included in this study. The pixel size of these CT images is between 0.59mm^2 to 0.74mm^2 . The slice thickness and the spacing in z-direction were fixed at 0.75mm and 0.5mm respectively. The kidney region of interest which size was $152 \times 152 \times Z$ was extracted.

❖ Visual superiority

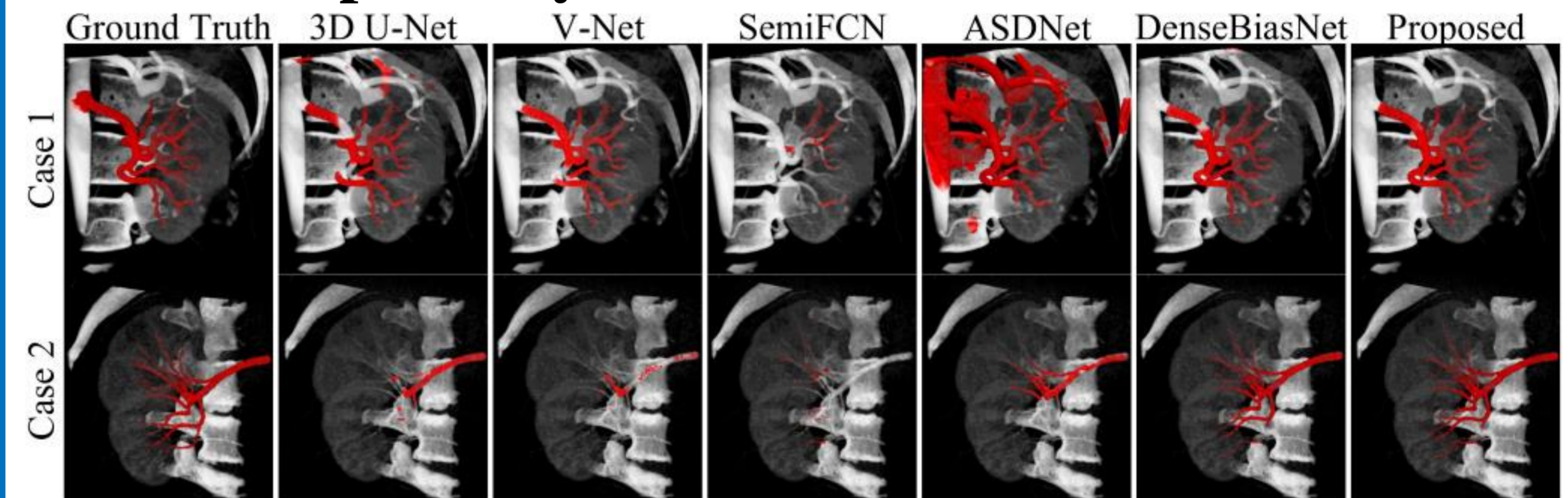


Fig.3 The visual superiority of our framework.

❖ Evaluation metrics advantages

Tab.1 The advantages of our method (DPA-DenseBiasNet) on each metrics.

Network	Dice	MCD	MSD
V-Net[8]	0.787(0.113)	2.872(2.196)	2.213(2.155)
3D U-Net[4]	0.750(0.162)	5.070(4.949)	4.385(4.208)
(semi)SemiFCN[3]	0.388(0.259)	8.772(10.085)	7.921(10.593)
(semi)ASDNet[9]	0.555(0.191)	8.557(5.124)	7.484(5.132)
DenseBiasNet	0.851(0.110)	2.478(2.090)	1.920(2.354)
(semi)Proposed	0.861(0.095)	1.976(1.394)	1.472(1.738)

❖ Training process improvement

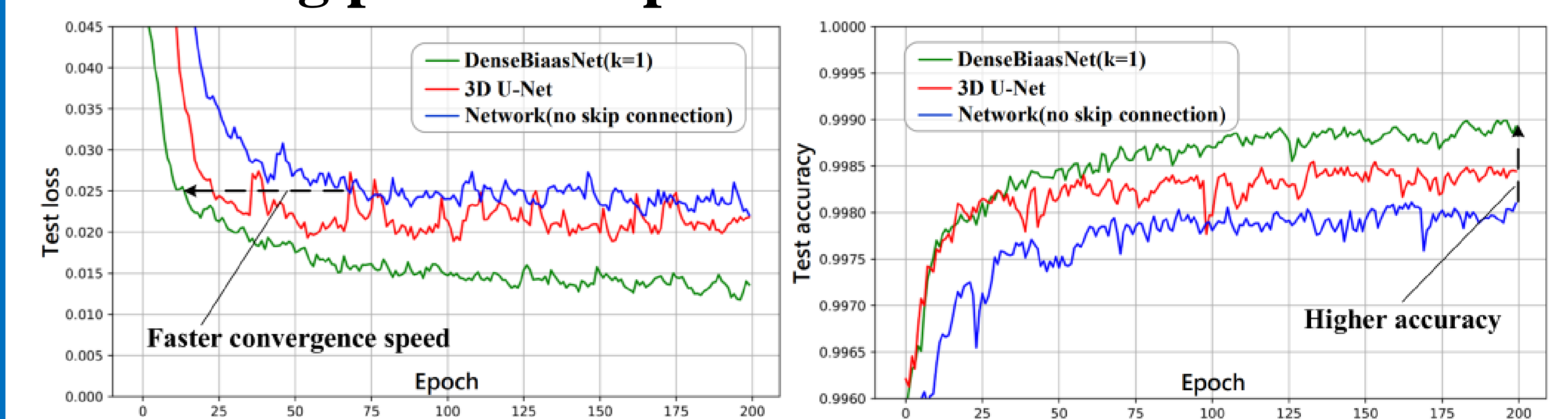


Fig.4 The improvement of the training process by the dense biased connection.

ACKNOWLEDGEMENTS

This research was supported by the National Key Research and Development Program of China (2017YFC0107903), National Natural Science Foundation under grants (31571001, 61828101), the Short-Term Recruitment Program of Foreign Experts (WQ20163200398), Key Research and Development Project of Jiangsu Province (BE2018749) and Southeast University Nanjing Medical University Cooperative Research Project (2242019K3DN08).